

MicroRNA-126 inhibits tumor cell invasion and metastasis by downregulating *ROCK1* in renal cell carcinoma

GUI-MING ZHANG¹, LEI LUO¹, XUE-MEI DING², DA-HAI DONG¹,
BIN LI¹, XIAO-CHENG MA¹ and LI-JIANG SUN¹

Departments of ¹Urology and ²Surgery, The Affiliated Hospital of Qingdao University,
Qingdao, Shandong 266003, P.R. China

Received May 26, 2015; Accepted April 2, 2016

DOI: 10.3892/mmr.2016.5160

Abstract. MicroRNAs (miRNAs) are involved in cancer development and progression. Renal cell carcinoma (RCC) frequently undergoes metastasis and has a high mortality rate. The current study measured miRNA-126 (miR-126) expression levels in 128 pairs of clear cell RCC and adjacent normal kidney tissue samples by reverse transcription-quantitative polymerase chain reaction, and analyzed the association between miR-126 and various clinicopathological parameters. In addition, cell proliferation, wound healing and cell invasion assays were conducted using RCC cells overexpressing miR-126. Potential miR-126 target genes and the signaling pathways that may be regulated by miR-126 were then examined. miR-126 expression was significantly reduced in patients with metastatic RCC compared with patients without metastasis. Consistently, overexpression of miR-126 in RCC cells significantly inhibited cell proliferation, migration and invasion *in vitro* compared with negative control miRNA. A luciferase reporter assay demonstrated that miR-126 targets Rho associated coiled-coil containing protein kinase 1 (*ROCK1*) by directly binding the 3'-untranslated region. Furthermore, western blotting identified miR-126 as an important regulator of the AKT and extracellular signal-regulated 1/2 signaling pathways. The results of the present study indicate that miR-126 inhibits RCC cell proliferation, migration and invasion by downregulating *ROCK1*. These findings suggest that miR-126 may be valuable as a potential target for therapeutic intervention in RCC.

Introduction

Renal cell carcinoma (RCC) is the predominant kidney neoplasm and accounts for 2-3% of all adult tumors. Clear cell RCC (ccRCC) is the most frequent pathological subtype of RCC (1). Approximately 30% of RCC patients have developed metastases at the time of diagnosis and metastasis occurs in 30-50% of patients with RCC following complete resection of the primary tumor (2). While recent therapeutic developments have improved the overall survival of patients with metastatic RCC, long-term prognosis remains poor (3). Thus, a greater understanding of the mechanisms underlying RCC development and progression is required. Furthermore, identification of novel RCC markers would aid the tailoring of treatment strategies and facilitate improved follow-up post-therapy.

MicroRNA-126 (miR-126) is of interest in cancer therapeutics due to its association with various types of tumor. miR-126 functions as a tumor suppressor in colorectal cancer (4), and inhibits the cell growth, invasion and migration of osteosarcoma cells (5). In addition, loss of miR-126 expression may promote prostate cancer progression and is associated with biochemical recurrence in patients undergoing radical prostatectomy (6). However, Otsubo *et al* (7) previously reported that overexpression of miR-126 may promote gastric carcinogenesis. A previous bioinformatic analysis identified miR-126 as a potential marker of metastasis during RCC progression (8). Another previous study reported a positive association between miR-126 expression and cancer-specific survival in ccRCC (9). However, the underlying mechanism of the regulation of RCC pathophysiology by miR-126 expression remains to be elucidated.

The current study determined the miR-126 expression levels in 128 ccRCC tissue samples matched with adjacent normal kidney tissue using reverse transcription-quantitative polymerase chain reaction (RT-qPCR). No difference was detected in miR-126 expression levels between ccRCC and normal kidney tissue samples. However, miR-126 expression was significantly reduced in metastatic ccRCC tissues compared with non-metastatic RCC tissues. In addition, the current study demonstrated that overexpression of miR-126 in RCC cells inhibits cell proliferation, migration and invasion *in vitro*. Furthermore, Rho associated coiled-coil containing

Correspondence to: Dr Li-Jiang Sun, Department of Urology, The Affiliated Hospital of Qingdao University, 16 Jiangsu Road, Qingdao, Shandong 266003, P.R. China
E-mail: sljiang999@126.com

Key words: microRNA-126, renal cell carcinoma, Rho associated coiled-coil containing protein kinase 1, cell invasion

protein kinase 1 (*ROCK1*) was identified as a target gene through which miR-126 promotes these inhibitory functions.

Materials and methods

Patient samples. A total of 128 pairs of ccRCC tissue and matched adjacent normal kidney tissue samples were obtained from the Department of Urology at The Affiliated Hospital of Qingdao University (Qingdao, China). The clinicopathological characteristics of all patients were retrieved from the medical database. The protocol of the current study was approved by the Institutional Research Review Board at The Affiliated Hospital of Qingdao University and written informed consent was obtained from all patients included in the study.

Cell lines and cell culture. Human RCC cell lines were obtained from the Institute of Cell Research of the Chinese Academy of Sciences (Shanghai, China) and cultured at 37°C in 5% CO₂ atmosphere. The cell lines 786-O and 769-P (derived from primary renal cell carcinoma) were grown in RPMI-640 medium (Hyclone; GE Healthcare Life Sciences, Logan, UT, USA). ACHN cells and Caki-1 cells (derived from metastatic renal cell carcinoma) were cultured in minimal essential medium and McCoy's 5A medium (Gibco; Thermo Fisher Scientific, Inc., Waltham, MA, USA). All media were supplemented with 10% fetal bovine serum (FBS; Hyclone; GE Healthcare Life Sciences).

Cell transfection. The miR-126-3p mimic and non-specific microRNA (miRNA) control (NC) were synthesized by Guangzhou RiboBio Co., Ltd. (Guangzhou, China). The sequences of the miR-126-3p mimic were as follows: Sense, 5'-UCGUACCGUGAGUAAUAAUGCG-3'; and anti-sense, 5'-CAUUUUUACUCACGGUACGAUU-3'. For transfection, cells were cultured in 6-well plates overnight followed by transfection of miR-126 mimic or NC using riboFECT™ CP reagent (Guangzhou RiboBio Co., Ltd.) according to the manufacturer's protocol. After 48 h, the cells were harvested for further experiments.

RNA extraction and RT-qPCR. Total RNA was extracted from tissues or cultured cells using TRIzol reagent (Thermo Fisher Scientific, Inc.) and used to synthesize first-strand cDNA with the RevertAid First-Strand cDNA synthesis kit (Thermo Fisher Scientific, Inc.). For mRNA analysis, RT-qPCR was performed using the Power SYBR Green PCR Master mix (Thermo Fisher Scientific, Inc.), an ABI 7900HT Fast Real-Time PCR system and the following protocol: 25°C for 5 min, 42°C for 1 h and 70°C for 5 min. β -actin levels were measured as an internal control. The primer sequences (Sangon Biotech, Co., Ltd., Shanghai, China) used were as follows: Forward, 5'-GGTGGTTCGGTTGGGTATTT-3' and reverse, 5'-AATGGTGCTACAGTGTCTCG-3' for *ROCK1*; and forward, 5'-ACCGAGCGCGGCTACAG-3' and reverse, 5'-CTTAATGTCACGCACGATTTC-3' for β -actin. Expression levels of miR-126 were measured using the LNA-miRNA Detection kit (Roche Diagnostics, Basel, Switzerland) and observed reduced expression levels of miR-126 in all four cell lines (U6 small nuclear RNA served as an internal control). The expression levels of mRNA or miR-126 were denoted as mRNA/ β -actin

(2^{- $\Delta\Delta$ Cq}) or miR-126/U6 (Δ Cq) (10). Following detection of expression levels in all four cell types, 786-O and ACHN cells were selected for use in subsequent experiments to represent primary and metastatic RCC, respectively.

Vector construction and luciferase assays. The *ROCK1* 3'-untranslated region (UTR) luciferase reporter vector was generated by introducing the wild-type *ROCK1* 3'-UTR, which carries a putative miR-126 binding site, into the psiCHECK2 vector (psi-ROCK1-WT; Promega Corporation, Madison, WI, USA). A corresponding control vector carrying the mutant *ROCK1* 3'-UTR was also constructed (psi-ROCK1-Mut). All vectors were validated by sequencing (Sangon Biotech, Co., Ltd.).

Co-transfection of psi-ROCK1-WT, psi-ROCK1-Mut or empty vector and miRNA mimics into 786-O cells was performed using Lipofectamine 3000 reagent (Invitrogen; Thermo Fisher Scientific, Inc.) according to the manufacturer's protocol. Following incubation for 48 h, the cells were lysed using passive lysis buffer (Promega Corporation). The dual-luciferase assay was then performed according to the manufacturer's protocols (Dual-Luciferase Reporter Assay System; Promega Corporation) and a Synergy H4 microplate reader (Bio-Tek Instruments, Inc., Winooski, VT, USA) was used. Luciferase activities were expressed as the ratio of firefly to *Renilla* luciferase activity. All experiments were performed in triplicate.

Cell proliferation assays. Cell proliferation was assessed using cell counting kit-8 (CCK-8) and EdU assays. For the CCK-8 assay, 786-O and ACHN cells were seeded in 96-well plates for 24 h, then transfected with miR-126 mimics or NC. After 24 h, cell viability was measured using the CCK-8 assay (Dojindo Molecular Technologies, Inc., Shanghai, China) according to the manufacturer's protocols. Absorbance at a wavelength of 450 nm was determined with a Synergy H4 microplate reader (Bio-Tek Instruments, Inc.).

For the EdU assay, 786-O and ACHN cells were incubated in EdU solution (1:5,000; Guangzhou RiboBio Co., Ltd.) for 2 h, then harvested and stained using the Cell-Light EdU Apollo 643 *in vitro* Flow Cytometry kit (Guangzhou RiboBio Co., Ltd.) according to the manufacturer's instructions. Cells were fixed with 0.5% Triton X-100 (Beijing Solarbio Science & Technology Co., Ltd., Beijing, China) and analyzed by flow cytometry (Cytomics FC 500 MPL; Beckman Coulter, Inc., Brea, CA, USA).

Wound healing assay. Cells were cultured in a monolayer in 6-well plates. The monolayer was manually scratched with a pipette tip to form a wound and cells were observed under inverted microscope (IX51; Olympus Corporation, Co., Ltd.) at 0 and 12 h time points.

Cell invasion assay. A Transwell chamber assay (BD Biosciences, Franklin Lakes, NJ, USA) was performed to observe cellular invasion *in vitro*. Briefly, the upper chamber was coated with 60 μ l Matrigel (BD Biosciences) diluted with serum-free medium (1:50). Cells were then seeded into the upper chamber in 200 μ l serum-free medium at a density of 4x10⁴ cells/chamber. The lower chamber was filled with 750 μ l medium containing

10% FBS. Following incubation at 37°C for 48 h, cells were fixed with 4% polyoxymethylene (Shanghai Macklin Reagent Co., Ltd., Shanghai, China) for 10 min, followed by staining with 0.5% crystal violet (Shanghai Macklin Reagent Co., Ltd.) for 30 min. Cells that did not invade through the pores were wiped away with a cotton swab. Invaded cells were counted using an inverted microscope. The experiment was repeated three times.

Protein extraction and western blot analysis. Total cellular proteins were extracted using the CellLytic Extraction kit containing protease inhibitors (Sigma-Aldrich, St. Louis, MO, USA) and quantified using a Pierce BCA Protein Assay kit (Thermo Fisher Scientific, Inc.). Equal quantities (30-50 µg) of protein were separated using 10% sodium dodecyl sulfate-polyacrylamide gel electrophoresis (at 100 V for 90 min) and transferred to polyvinylidene fluoride membranes. Membranes were blocked using 5% skim milk and then incubated with monoclonal rabbit anti-ROCK1 (1:500; Abcam, Cambridge, UK; cat. no. ab45171), monoclonal rabbit AKT (cat. no. 4691), monoclonal rabbit phosphorylated (p)-AKT (cat. no. 4060), monoclonal mouse extracellular signal-regulated kinase 1/2 (ERK1/2; cat. no. 4696) and monoclonal rabbit p-ERK1/2 (cat. no. 4370) all at 1:1,000 dilution (Cell Signaling Technology, Inc., Danvers, MA, USA) primary antibodies at 4°C overnight. Mouse monoclonal GAPDH (1:3,000; cat. no. ab8245; Abcam) served as a loading control. The membranes were then washed with phosphate-buffered saline (Thermo Fisher Scientific, Inc.) and then incubated for 2 h at room temperature with horseradish peroxidase (HRP)-conjugated secondary antibodies as follows: Goat anti-mouse IgG HRP (cat. no. sc-2031) and goat anti-rabbit IgG HRP (cat. no. sc-2030; 1:6,000; Santa Cruz Biotechnology, Inc., Dallas, TX, USA). Signals were visualized using the ECL Plus Western Blotting system (Thermo Fisher Scientific, Inc.) and blots were visualized with the ImageQuant LAS 4000 system (GE Healthcare Life Sciences, Uppsala, Sweden).

Immunohistochemistry (IHC). IHC staining of paraffin-embedded specimens was performed as previously described (11). Briefly, following antigen retrieval, 5-µm sections were soaked with 3% H₂O₂-methanol (Shanghai Macklin Reagent Co., Ltd.) for 15 min to block peroxidase activity, and incubated with 10% normal goat serum (Shanghai Haoran Bio Technologies Co., Ltd., Shanghai, China) to block non-specific protein binding. Sections were then incubated with anti-ROCK1 primary antibody (1:100), followed by rabbit anti-mouse HRP-labeled antibody (cat. no. GK500705; Shanghai Universal Biotech Co., Shanghai, China). A BX51 microscope (Olympus Corporation) was used to visualize the slides and ROCK1 staining was scored as 0, 1, 2 and 3, as previously described (12).

Statistical analysis. Student's t-test or analysis of variance was performed to compare differences between continuous variables. Differences between categorical variables were analyzed using the χ^2 test. Two-sided P<0.05 was considered to indicate a statistically significant difference. All statistical analyses were performed using SPSS software version 20.0 (IBM SPSS, Armonk, NY, USA) and data are presented as means \pm standard deviation.

Table I. Clinicopathological characteristics of 128 clear cell renal cell carcinoma patients.

Clinicopathological feature	n	(%)
Age (years)		
<65	108	84.4
≥65	20	15.6
Gender		
Male	95	74.2
Female	33	25.8
Body mass index		
<25 kg/m ²	91	71.1
≥25 kg/m ²	37	28.9
Smoking status		
Never	84	65.6
Ever/current	44	34.3
Hypertension		
No	84	65.6
Yes	44	34.3
Diabetes		
No	89	69.5
Yes	39	30.5
Tumor stage		
1	96	75.0
2	19	14.8
3	8	6.3
4	5	3.9
Lymph node stage		
N0	121	94.5
N1	7	5.5
Metastasis stage		
M0	102	79.7
M1	26	20.3
Clinical stage		
I	84	65.6
II	11	8.6
III	7	5.5
IV	26	20.3
Fuhrman grade		
1	5	3.9
2	55	43.0
3	54	42.2
4	14	10.9

Results

miR-126 expression is reduced in ccRCC tissue with metastasis. The clinicopathological characteristics of the 128 patients with ccRCC are presented in Table I. miR-126 expression was detected in tumor and matched adjacent normal kidney tissues from each of the 128 patients using RT-qPCR. No significant difference in miR-126 expression was observed between

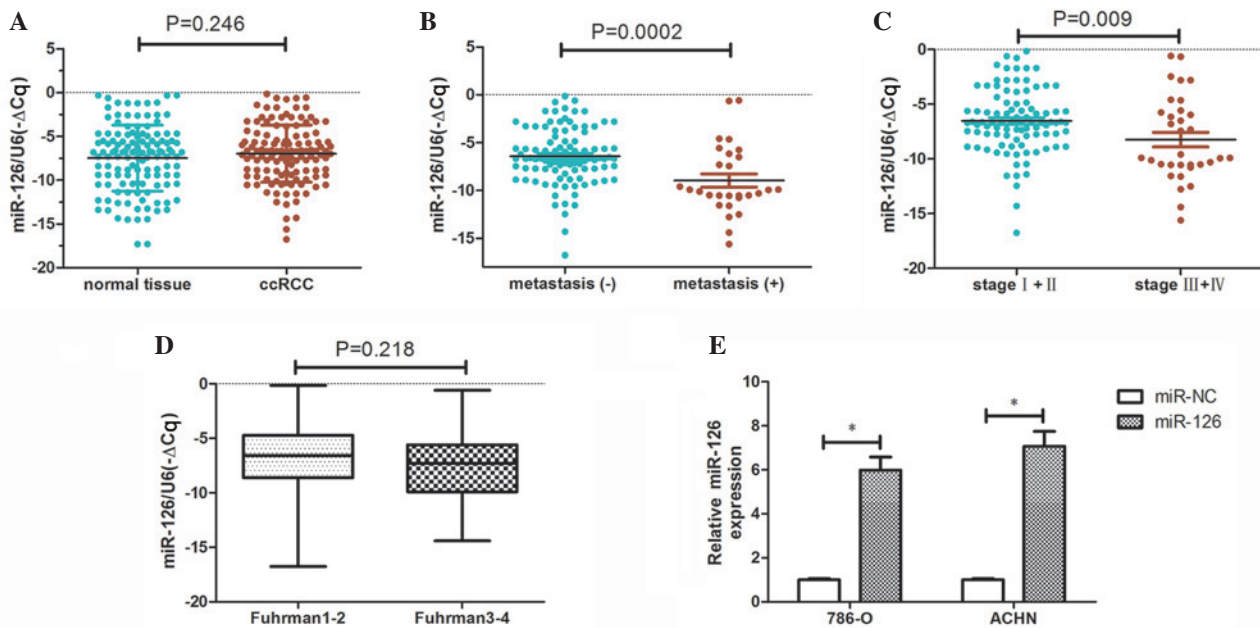


Figure 1. miR-126 expression profiles in ccRCC and normal kidney tissue samples, and RCC cells. (A) miR-126 expression in ccRCC tissue and adjacent normal kidney tissue. MiR-126 expression in (B) ccRCC tissue with metastasis compared with tissue without metastasis, and (C) stage III/IV disease compared with stage I/II disease. (D) Difference in miR-126 expression between low and high grade disease. (E) Expression of miR-126 in 786-O and ACHN cells transfected with miR-126 mimics. * $P < 0.05$, comparison indicated by brackets. miR, microRNA; ccRCC, clear cell renal cell carcinoma; NC, negative control.

ccRCC tissues and benign samples ($P = 0.246$; Fig. 1A). In addition, the potential association between miR-126 expression and clinicopathological variables was determined. Of the 128 patients, 7 presented with lymph node metastasis and 26 with distant metastasis. Further analyses demonstrated that the expression levels of miR-126 were significantly lower in patients with metastasis (lymph node or distant metastasis) compared with those without metastasis ($P = 0.0002$; Fig. 1B). Similarly, patients with stage III/IV disease exhibited significantly reduced expression of miR-126 compared with stage I/II disease ($P = 0.009$; Fig. 1C). However, no difference in miR-126 expression was observed between low grade and high grade tumors ($P = 0.218$; Fig. 1D). These findings suggest that suppression of miR-126 expression may be associated with ccRCC progression.

miR-126 overexpression inhibits RCC cell proliferation *in vitro*. The levels of miR-126 expression were determined in 4 human RCC cell lines (786-O, 769-P, ACHN and Caki-1; data not presented). ACHN and 786-O cells were selected for further analysis.

Transfection with miR-126 mimic was used to overexpress miR-126 in 786-O and ACHN cells, and transfection successfully increased miR-126 mRNA levels in miR-126 overexpressing cells compared with NC ($P < 0.05$; Fig. 1E). Changes to RCC cell proliferation following miR-126 overexpression were assessed by CCK-8 and EdU assays. As demonstrated in Fig. 2A, proliferation was significantly reduced in 786-O-miR-126 and ACHN-miR-126 cells compared with relevant NC control cells ($P < 0.05$). Flow cytometry analysis demonstrated that the proportion of EdU-positive cells in 786-O-miR-126 and ACHN-miR-126 cells was markedly decreased compared with the relevant controls (Fig. 2B). These findings suggest that miR-126 overexpression inhibits RCC cell proliferation *in vitro*.

miR-126 over-expression inhibits RCC cell invasion and migration *in vitro*. The present study determined whether miR-126 overexpression inhibits RCC cell migration and invasion. Transwell chamber assays demonstrated that miR-126 overexpression significantly inhibited the invasive capacity of 786-O and ACHN cells compared with NC cells ($P < 0.05$; Fig. 2C). RCC cell motility was assessed using a wound-healing assay. Cell migration of 786-O-miR-126 and ACHN-miR-126 was markedly reduced compared with the relevant NC controls 12 h after wound creation (Fig. 2D). These results indicate that miR-126 overexpression inhibits RCC cell invasion and migration *in vitro*.

miR-126 suppresses *ROCK1* expression by directly targeting the 3'-UTR. Bioinformatics screening was performed (www.targetscan.org; www.mirbase.org) to identify potential miR-126 target genes. The *ROCK1* mRNA 3'UTR contains a conserved binding site for miR-126. The protein and mRNA expression levels of *ROCK1* in 786-O-miR-126, ACHN-miR-126 and their respective control cells were then determined. Compared with controls, the *ROCK1* mRNA expression levels were significantly downregulated ($P < 0.05$; Fig. 3A) and the protein expression levels were also downregulated (Fig. 3B), suggesting that miR-126 suppresses *ROCK1* expression in RCC cells.

Luciferase reporter vectors carrying the human *ROCK1* 3'-UTR were constructed with either the wild-type miR-126 binding sequence (psi-*ROCK1*-WT) or a mutant sequence (psi-*ROCK1*-Mut) to which miR-126 does not bind (Fig. 3C). Following co-transfection of 786-O cells with the reporters and miR-126 mimic, the relative luciferase activity in psi-*ROCK1*-WT-transfected cells was decreased by 26% compared with NC cells ($P < 0.05$; Fig. 3D). No significant effect was observed with the mutant reporters. These findings

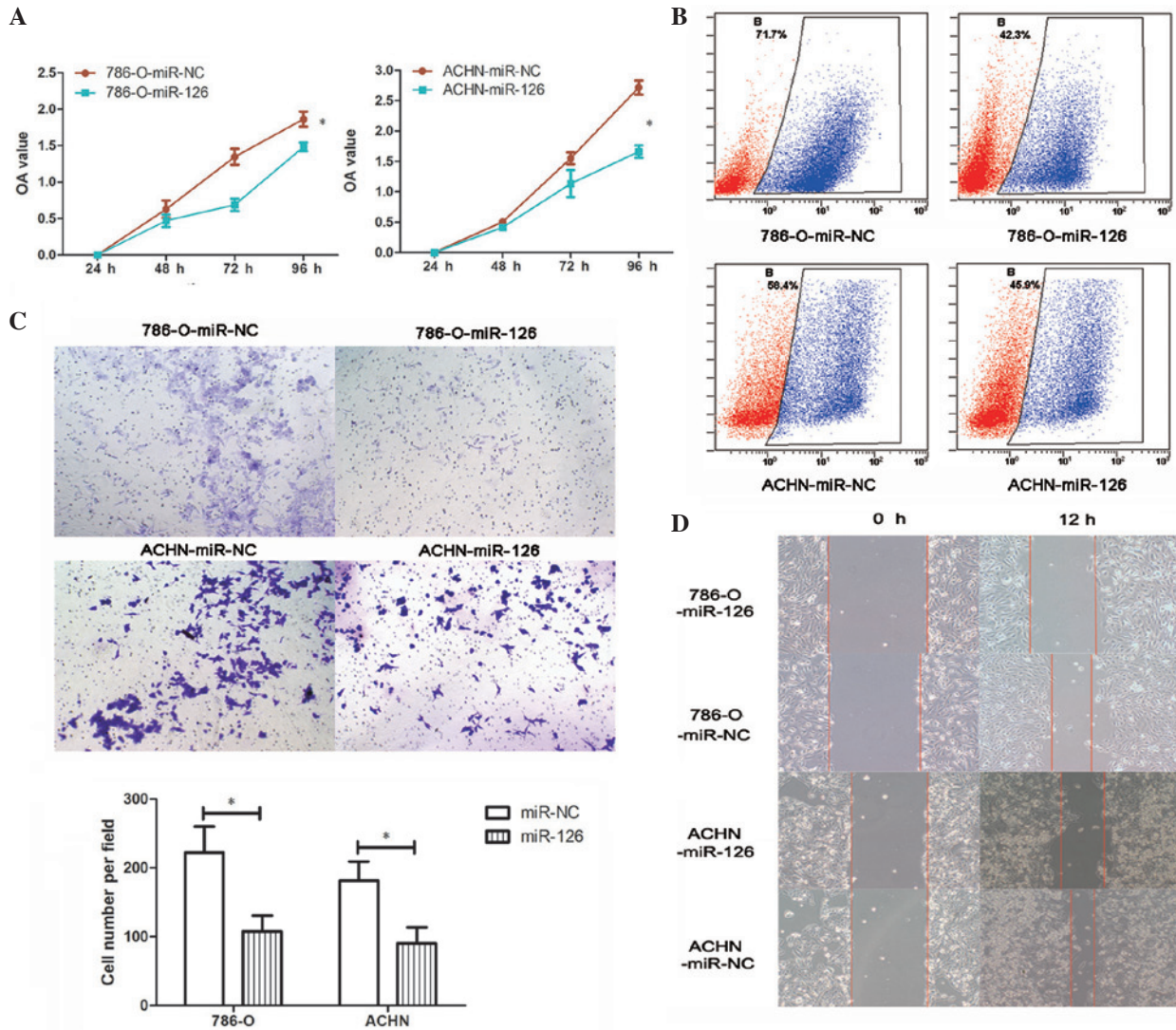


Figure 2. Overexpression of miR-126 inhibits cell proliferation, migration, and invasion in renal cell carcinoma cells *in vitro*. (A) Cell counting kit-8 assays were performed to measure cell proliferation in 786-O and ACHN cells. Data are presented as the mean \pm standard deviation of the OD value detected at 450 nm from three independent experiments. (B) Cell proliferation was analyzed in 786-O and ACHN cells using EdU assay by flow cytometry. (C) Transwell and (D) wound healing assays were performed following miR-126 overexpression in the indicated cells. * $P < 0.05$, comparison indicated by brackets. miR, microRNA; NC, negative control OD, optical density.

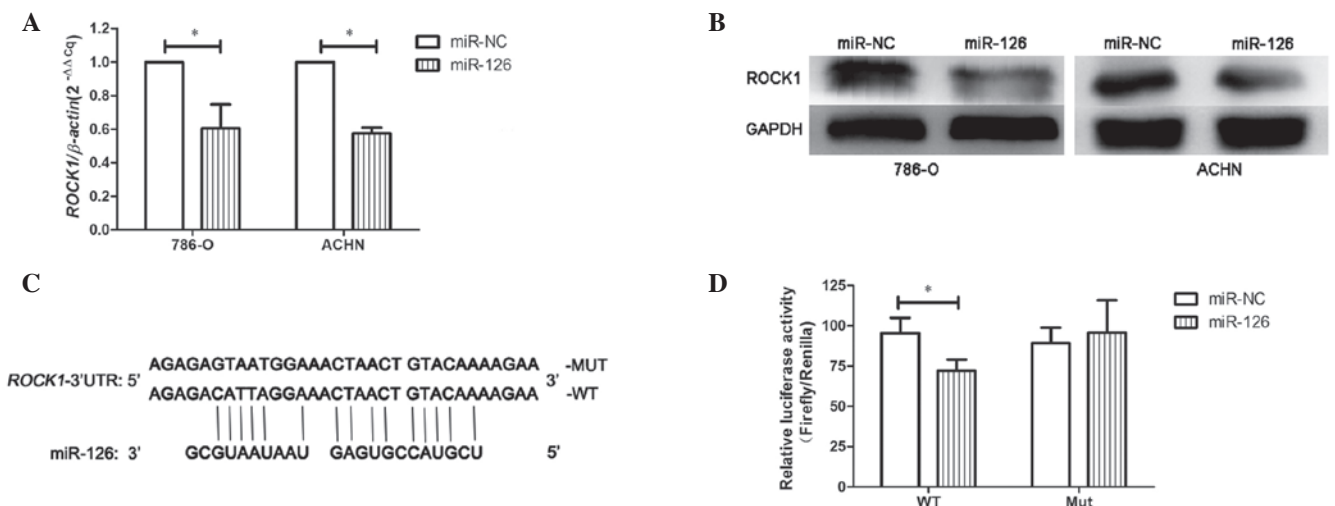


Figure 3. MiR-126 suppresses *ROCK1* expression by directly targeting its 3'-UTR. *ROCK1* expression in 786-O and ACHN cells at the (A) mRNA and (B) protein level. (C) Schematic representation of the luciferase reporter, which carried the wild-type or mutant *ROCK1*-3'-UTR. (D) Relative luciferase activity in wild-type *ROCK1*-3'-UTR and mutant *ROCK1*-3'-UTR reporter-transfected cells. * $P < 0.05$, comparison indicated by brackets. miR, microRNA; NC, negative control; ROCK, Rho associated coiled-coil containing protein kinase 1; 3'UTR, 3' untranslated region.

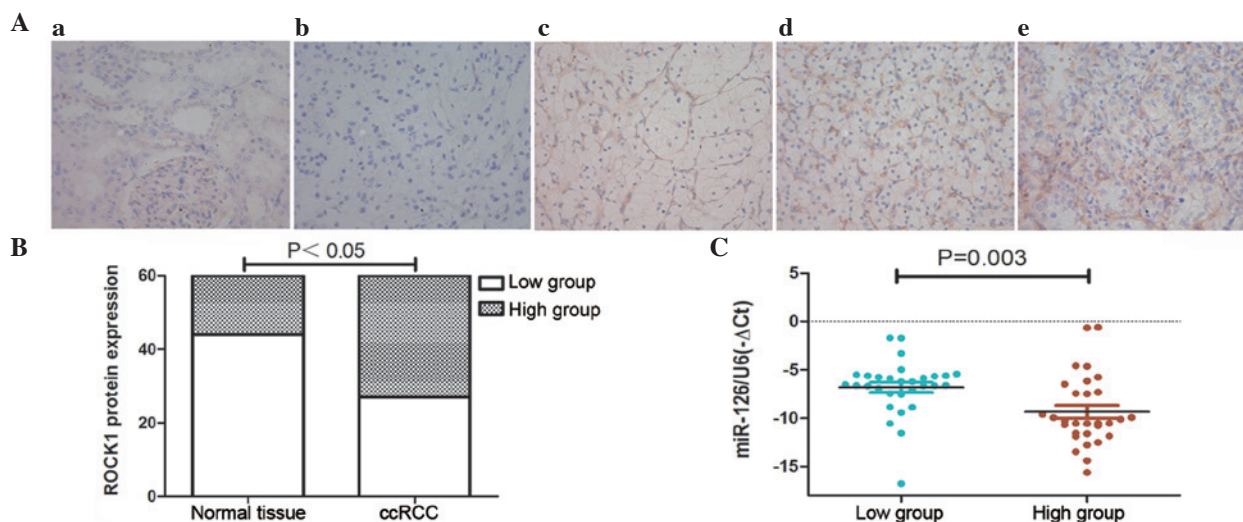


Figure 4. Upregulation of *ROCK1* is inversely correlated with miR-126 expression in ccRCC tissue. (A) Immunohistochemical (IHC) staining of *ROCK1* in ccRCC tissue compared with adjacent normal kidney tissue (magnification, $\times 400$). The staining intensity was represented as follows: (a) normal kidney tissue, score 0; (b) ccRCC, score 0; (c) ccRCC, score 1; (d) ccRCC, score 2; (e) ccRCC, score 3; (B) Comparison of *ROCK1* expression based upon IHC staining. (C) Correlation analysis of *ROCK1* expression and miR-126 levels in 60 ccRCC tissue samples. *ROCK1*, Rho associated coiled-coil containing protein kinase 1; ccRCC, clear cell renal cell carcinoma; miR, microRNA.

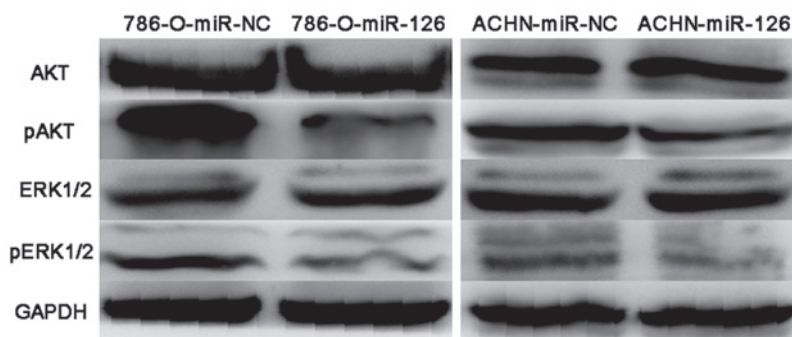


Figure 5. Overexpression of miR-126 in renal cell carcinoma (RCC) cells results in changes in the AKT and ERK1/2 signaling pathways. Western blot analyses of AKT, pAKT, ERK1/2, and pERK1/2 levels in miR-126 overexpressing RCC cells. Western blot analyses demonstrated decreased p-AKT and p-ERK1/2 levels in miR-126 overexpressing RCC cells, whereas total AKT and ERK1/2 levels were not affected. miR, microRNA; NC, negative control; p, phosphorylated; ERK, extracellular signal-regulated kinase.

suggest that miR-126 inhibits *ROCK1* expression in RCC cells by directly targeting the *ROCK1* 3'-UTR.

Upregulation of ROCK1 is inversely correlated with miR-126 expression in ccRCC tissue samples. The present study examined whether *ROCK1* protein expression levels were associated with miR-126 expression in ccRCC tissue samples. IHC staining was performed on 60 paired ccRCC and adjacent normal kidney tissue samples (randomly selected from the 128 patients in Table I). The expression levels of *ROCK1* were classified into low (scores of 0 and 1) and high (scores of 2 and 3) groups according to IHC staining (Fig. 4A). *ROCK1* was upregulated in ccRCC tissue compared with adjacent normal kidney tissue ($P < 0.05$; Fig. 4A and B). Furthermore, the association between *ROCK1* expression and miR-126 levels in ccRCC tissues was analyzed, and the results demonstrated that high levels of *ROCK1* were more likely to be observed in ccRCC with low levels of miR-126 ($P < 0.003$; Fig. 4C), suggesting that inhibition of miR-126 may increase *ROCK1* expression in ccRCC tissues.

miR-126 is an important regulator of the AKT and ERK1/2 signaling pathways. Finally, the present study investigated whether miR-126 regulates the AKT and ERK1/2 signaling cascades, as these pathways are important in cancer initiation and development. Western blotting did not demonstrate any observable changes in total AKT and ERK1/2 protein expression levels following miR-126 overexpression in RCC cells. However, decreased levels of AKT and ERK1/2 phosphorylation were observed in 786-O-miR-126 and ACHN-miR-126 cells compared with the relevant controls (Fig. 5). The results suggested that the inhibitory activity of miR-126 in RCC may be at least partially mediated by regulation of the AKT and ERK1/2 signaling pathways.

Discussion

Various studies have identified associations between miRNAs and tumor development and progression. Furthermore, numerous miRNAs have been termed 'oncomiRs', and function as cancer biomarkers and/or regulators of important biological

processes. Among these oncomiRs, miR-126 has previously been implicated in the carcinogenesis of multiple types of cancer (5,13-15). However, while the pattern of miR-126 and miR-21 expression may be a predictor of cancer-specific survival in ccRCC (9), the specific effects exerted by miR-126 in RCC, and the underlying mechanisms involved, remain to be elucidated. The present study demonstrated an inhibitory effect of miR-126 on the proliferation, migration and invasion of RCC cells, and, to the best of our knowledge, is the first report to identify *ROCK1* as a novel target gene of miR-126.

Accumulating evidence indicates that miR-126 exerts anti-cancer effects. Overexpression of miR-126 in colon cancer cells has been demonstrated to result in a reduction in cell growth (16), while increased miR-126 inhibited the proliferation of osteosarcoma, small cell lung cancer, and stromal cells from giant cell bone tumors (5,17,18). Elevated miR-126 levels also impaired cellular migration and invasion in these previous studies. Other reports have demonstrated similar findings in colon cancer, breast cancer, pancreatic cancer and chronic myeloid leukemia (4,19-21). Consistently, high miR-126 expression has been associated with favorable clinical outcomes in non-small cell lung cancer (15) and prostate cancer (6). Together, these findings suggest that miR-126 functions as a tumor suppressor. However, another study reported contrasting findings. miR-126 may contribute to the carcinogenesis of acute myeloid leukemia by inhibiting cell apoptosis and promoting cell proliferation (22). Overexpression of miR-126 may also enhance growth of gastric cancer cells by inhibiting SRY (sex determining region Y)-box 2 (*SOX2*) expression (7). The present study supports tumor suppressor activity for miR-126 in RCC, consistent with a previous report that identified decreased levels of miR-126 in RCC tissues (9). Furthermore, the previous study demonstrated that miR-126 expression was reduced further in tumor tissue samples of higher stage and grade (9). The variable effects of miR-126 may be partially explained by the heterogeneity of tumors of different origins. However, further studies are required to elucidate the precise mechanism by which miR-126 functions in RCC and other types of cancer.

miRNAs regulate a diverse range of biological processes by specifically binding and inducing cleavage of target mRNAs, or inhibiting their translation (23,24). Several important miR-126 target genes have been previously identified, including *p38*, *SOX2*, C-X-C chemokine receptor type 4 and vascular endothelial growth factor (4,7,13,14). The current study demonstrated that overexpression of miR-126 reduced *ROCK1* protein expression levels and *ROCK1* 3'-UTR luciferase activity. Furthermore, reporter assays using a mutant sequence of the *ROCK1* 3'-UTR demonstrated that miR-126 post-transcriptionally regulates *ROCK1* by directly binding its 3'-UTR. As a key effector kinase downstream of Rho GTPase, *ROCK1* activity is essential for the cytoskeletal reorganization process required for cell motility and invasion (25,26). Accumulating evidence suggests that *ROCK1* contributes to invasion and metastasis in various types of cancer (27-29). The present study demonstrated that miR-126 levels are reduced in metastatic ccRCC tissues. Furthermore, overexpression of miR-126 inhibits cell migration and invasion, likely via targeting *ROCK1*. The results from the current study provide novel insights into the mechanisms underlying RCC progression and metastasis.

The current study also identified that miR-126 regulates the AKT and ERK1/2 signaling pathways, which are important during carcinogenesis. Previous reports suggest an association between AKT and ERK1/2, and *ROCK1* signal transduction. A previous study observed that *ROCK1* protein expression levels were higher in prostate cancer tissue samples compared with corresponding paracancerous tissue samples, and was associated with p-mitogen-activated protein kinase (MAPK) and p-AKT levels (30). Another previous study identified an association between *ROCK1* and increased ERK/MAPK activation in transgenic mice (31). The current study demonstrated that miR-126 overexpression decreases phosphorylated AKT and ERK1/2 levels without altering the total AKT and ERK1/2 protein expression levels. Thus, the present study hypothesizes that downregulation of *ROCK1* by miR-126 may result in subsequent regulation of AKT and ERK1/2 phosphorylation.

The results of the current study indicated that *ROCK1* is upregulated in ccRCC tissue compared with adjacent normal kidney tissue, whereas no significant difference in miR-126 expression was observed in ccRCC tissues compared with benign samples. However, the expression of *ROCK1* was detected by IHC staining in 60 paired ccRCC and adjacent normal kidney tissue samples. The sample size was relatively small and there may be selection bias in the analysis. Furthermore, miRNAs exert their functions by regulating target genes. It is understood that one target gene may be regulated by different miRNAs. These target genes and miRNAs, as well as other transcription factors, constitute a complex network involved in various cellular processes. The signals and mechanisms that control miRNA transcriptional regulation remain unknown. In addition to miR-126, other factors may regulate the expression of *ROCK1* in ccRCC tissue and adjacent normal kidney tissue. Thus, the complex regulatory network through which miR-126 functions, and the importance of *ROCK1* expression and function in RCC carcinogenesis, requires further elucidation.

In conclusion, the current study identified an association between miR-126, and RCC progression and metastasis, suggesting that miR-126 may function as a tumor suppressor involved in RCC development. Thus, miR-126 may be a potential diagnostic biomarker and therapeutic target for RCC.

Acknowledgements

The current study was partly supported by the National Natural Science Foundation of China (grant no. NSFC 81502195) and the Medicine and Health Science Technology Development Project of Shandong Province (grant no. 2011HW028).

References

1. Chow WH and Devesa SS: Contemporary epidemiology of renal cell cancer. *Cancer J* 14: 288-301, 2008.
2. Rydzanicz M, Wrzesiński T, Bluysen HA and Wesoly J: Genomics and epigenomics of clear cell renal cell carcinoma: Recent developments and potential applications. *Cancer Lett* 341: 111-126, 2013.
3. Thillai K, Allan S, Powles T, Rudman S and Chowdhury S: Neoadjuvant and adjuvant treatment of renal cell carcinoma. *Expert Rev Anticancer Ther* 12: 765-776, 2012.
4. Liu Y, Zhou Y, Feng X, An P, Quan X, Wang H, Ye S, Yu C, He Y and Luo H: MicroRNA-126 functions as a tumor suppressor in colorectal cancer cells by targeting CXCR4 via the AKT and ERK1/2 signaling pathways. *Int J Oncol* 44: 203-210, 2014.

5. Jiang L, He A, Zhang Q and Tao C: MiR-126 inhibits cell growth, invasion and migration of osteosarcoma cells by downregulating ADAM-9. *Tumour Biol* 35: 12645-12654, 2014.
6. Sun X, Liu Z, Yang Z, Xiao L, Wang F, He Y, Su P, Wang J and Jing B: Association of microRNA-126 expression with clinicopathological features and the risk of biochemical recurrence in prostate cancer patients undergoing radical prostatectomy. *Diagnostic Pathol* 8: 208, 2013.
7. Otsubo T, Akiyama Y, Hashimoto Y, Shimada S, Goto K and Yuasa Y: MicroRNA-126 inhibits SOX2 expression and contributes to gastric carcinogenesis. *PLoS One* 6: e16617, 2011.
8. Khella HW, White NM, Faragalla H, Gabril M, Boazak M, Dorian D, Khalil B, Antonios H, Bao TT, Pasic MD, *et al*: Exploring the role of miRNAs in renal cell carcinoma progression and metastasis through bioinformatic and experimental analyses. *Tumour Biol* 33: 131-140, 2012.
9. Vergho D, Kneitz S, Rosenwald A, Scherer C, Spahn M, Burger M, Riedmiller H and Kneitz B: Combination of expression levels of miR-21 and miR-126 is associated with cancer-specific survival in clear-cell renal cell carcinoma. *BMC Cancer* 14: 25, 2014.
10. Zhang GM, Bao CY, Wan FN, Cao DL, Qin XJ, Zhang HL, Zhu Y, Dai B, Shi GH and Ye DW: MicroRNA-302a suppresses tumor cell proliferation by inhibiting AKT in prostate cancer. *PLoS One* 10: e0124410, 2015.
11. Qin X, Zhang H, Ye D, Dai B, Zhu Y and Shi G: B7-H3 is a new cancer-specific endothelial marker in clear cell renal cell carcinoma. *Oncotargets* 6: 1667-1673, 2013.
12. Liu X, Choy E, Hornicek FJ, Yang S, Yang C, Harmon D, Mankin H and Duan Z: ROCK1 as a potential therapeutic target in osteosarcoma. *J Orthop Res* 29: 1259-1266, 2011.
13. Liu B, Peng XC, Zheng XL, Wang J and Qin YW: MiR-126 restoration down-regulate VEGF and inhibit the growth of lung cancer cell lines in vitro and in vivo. *Lung Cancer* 66: 169-175, 2009.
14. Li X, Wang F and Qi Y: MiR-126 inhibits the invasion of gastric cancer cell in part by targeting Crk. *Eur Rev Med Pharmacol Sci* 18: 2031-2037, 2014.
15. Kim MK, Jung SB, Kim JS, Roh MS, Lee JH, Lee EH and Lee HW: Expression of microRNA miR-126 and miR-200c is associated with prognosis in patients with non-small cell lung cancer. *Virchows Arch* 465: 463-471, 2014.
16. Guo C, Sah JF, Beard L, Willson JK, Markowitz SD and Guda K: The noncoding RNA, miR-126, suppresses the growth of neoplastic cells by targeting phosphatidylinositol 3-kinase signaling and is frequently lost in colon cancers. *Genes Chromosomes Cancer* 47: 939-946, 2008.
17. Miko E, Margitai Z, Czimmerer Z, Várkonyi I, Dezsó B, Lányi A, Bacsó Z and Scholtz B: MiR-126 inhibits proliferation of small cell lung cancer cells by targeting SLC7A5. *FEBS Lett* 585: 1191-1196, 2011.
18. Zhou W, Yin H, Wang T, Liu T, Li Z, Yan W, Song D, Chen H, Chen J, Xu W, *et al*: MiR-126-5p regulates osteolysis formation and stromal cell proliferation in giant cell tumor through inhibition of PTHrP. *Bone* 66: 267-276, 2014.
19. Zhang Y, Yang P, Sun T, Li D, Xu X, Rui Y, Li C, Chong M, Ibrahim T, Mercatali L, *et al*: MiR-126 and miR-126* repress recruitment of mesenchymal stem cells and inflammatory monocytes to inhibit breast cancer metastasis. *Nature Cell Biol* 15: 284-294, 2013.
20. Hamada S, Satoh K, Fujibuchi W, Hirota M, Kanno A, Unno J, Masamune A, Kikuta K, Kume K and Shimosegawa T: MiR-126 acts as a tumor suppressor in pancreatic cancer cells via the regulation of ADAM9. *Mol Cancer Res* 10: 3-10, 2012.
21. Taverna S, Amodeo V, Saieva L, Russo A, Giallombardo M, De Leo G and Alessandro R: Exosomal shuttling of miR-126 in endothelial cells modulates adhesive and migratory abilities of chronic myelogenous leukemia cells. *Mol Cancer* 13: 169, 2014.
22. Li Z, Lu J, Sun M, Mi S, Zhang H, Luo RT, Chen P, Wang Y, Yan M, Qian Z, *et al*: Distinct microRNA expression profiles in acute myeloid leukemia with common translocations. *Proc Natl Acad Sci USA* 105: 15535-15540, 2008.
23. Bartel DP: MicroRNAs: Genomics, biogenesis, mechanism and function. *Cell* 116: 281-297, 2004.
24. Ambros V: The functions of animal microRNAs. *Nature* 431: 350-355, 2004.
25. Pinner S and Sahai E: PDK1 regulates cancer cell motility by antagonising inhibition of ROCK1 by RhoE. *Nat Cell Biol* 10: 127-137, 2008.
26. Narumiya S, Tanji M and Ishizaki T: Rho signaling, ROCK and mDia1, in transformation, metastasis and invasion. *Cancer Metastasis Rev* 28: 65-76, 2009.
27. Lin MT, Lin BR, Chang CC, Chu CY, Su HJ, Chen ST, Jeng YM and Kuo ML: IL-6 induces AGS gastric cancer cell invasion via activation of the c-Src/RhoA/ROCK signaling pathway. *Int J Cancer* 120: 2600-2608, 2007.
28. Schofield AV and Bernard O: Rho-associated coiled-coil kinase (ROCK) signaling and disease. *Crit Rev Biochem Mol Biol* 48: 301-316, 2013.
29. Sari I, Berberoglu B, Ozkara E, Oztuzcu S, Camci C and Demiryurek AT: Role of rho-kinase gene polymorphisms and protein expressions in colorectal cancer development. *Pathobiology* 80: 138-145, 2013.
30. Bu Q, Tang HM, Tan J, Hu X and Wang DW: Expression of RhoC and ROCK-1 and their effects on MAPK and Akt proteins in prostate carcinoma. *Zhonghua Zhong Liu Za Zhi* 33: 202-206, 2011 (In Chinese).
31. Shi J, Zhang YW, Yang Y, Zhang L and Wei L: ROCK1 plays an essential role in the transition from cardiac hypertrophy to failure in mice. *J Mol Cell Cardiol* 49: 819-828, 2010.